

# A hierarchical model for CNT and Cu-CNT composite interconnects: from density functional theory to circuit-level simulations

Jaehyun Lee<sup>1</sup>, Toufik Sadi<sup>1</sup>, Jie Liang<sup>2</sup>,  
Vihar P. Georgiev<sup>1</sup>, Aida Todri-Sanial<sup>2</sup>, and Asen Asenov<sup>1\*</sup>  
School of Engineering, University of Glasgow, Glasgow, UK<sup>1</sup>  
CNRS-LIRMM, University of Montpellier, Montpellier, France<sup>2</sup>

Metallic carbon nanotubes (CNTs) and Cu-CNT composites have been regarded for years as one of the promising candidates for the future interconnects to replace Cu. Due to CNTs' small effective mass and 1-D structure, and strong C-C bonding, they have a very high ampacity, a large mean free path ( $\lambda$ ), and excellent mechanical properties [1]. In this work, we have investigated the transport properties of CNT interconnects based on density functional theory (DFT) and compact model analysis. We also propose a hierarchical model to connect the DFT with circuit-level simulations.

We have used ATK [2] for DFT calculations involving the generalized gradient approximation (GGA). As the first step, a single-wall CNT (SWCNT) bundle as shown in Fig. 1 has been considered. In order to get optimal lattice constants, we have performed geometric optimization. All atoms are fully relaxed until the forces of any atom become less than 0.01 eV/Å. With the optimized atomistic structure, we have calculated the ballistic conductance ( $G_{bal}$ ) at 300 K using the non-equilibrium Green's function (NEGF) formalism.

Fig. 2 shows  $G_{bal}$  of SWCNT bundles and stand-alone SWCNTs. The difference between them, caused by the interaction with the adjacent SWCNTs, decreases as the diameter of CNTs ( $D_{CNT}$ ) increases.

Fig. 3 describes atomistic structures of iodine-doped SWCNT(24,0) and Cu-CNT(6,0) composite. In this work, the width (W) and height (H) of the local interconnect are assumed to be 8 and 16 nm, respectively, with reference to the ITRS node 2024 [3].

The resistance of the interconnect ( $R_w$ ) made of SWCNT bundles, the doped SWCNT, bulk Cu, and the Cu-CNT composite is plotted in Fig. 4. For bulk Cu, we do not consider the surface and grain boundary scattering effects. To calculate the diffusive conductance ( $G_{dif}$ ) from  $G_{bal}$ , we applied the mean free path approximation;  $G_{dif} = G_{bal}(1.0 + L/\lambda)^{-1}$ , where  $L$  is the

interconnect length. As can be seen in this figure, bulk Cu has smaller  $R_w$  for short interconnects. Due to the large  $\lambda$  of CNT, however,  $R_w$  of the SWCNT(6,0) becomes better as  $L$  increases. It is noticeable that Cu-CNT composite is characterized by combining the advantage of both Cu and CNT.

To calculate the propagation time delay ( $t_d$ ), we have considered a driver-interconnect-load system, as shown in Fig. 5.  $R_s$ ,  $C_s$ , and  $C_L$  are assumed to be 35 kΩ, 7 aF, and 14 aF, respectively [3]. The capacitance of the interconnect ( $C_w$ ) is defined by  $C_w^{-1} = C_E^{-1} + C_Q^{-1}$ , where  $C_E$  and  $C_Q$  are the classical electrostatic and quantum capacitances, respectively.  $C_Q$  was extracted using the following relationship [4];

$$C_Q = \frac{e^2}{4kT} \int D(E) \operatorname{sech}^2 \frac{E}{2kT} dE,$$

where  $D(E)$  is the density-of-states obtained from DFT-GGA calculations. The calculated  $C_Q$  values are summarized in Table 1.

We have calculated  $t_d$  by using the Elmore formula;  $t_d = 0.69\{R_s(C_s + C_L) + (R_w C_L + R_s C_w) + R_w C_w\}$ . Fig. 6 shows the dependence of  $t_d$  on  $L$  and  $C_E$ . In this calculation, we assumed that  $C_E$  does not rely on the interconnect material. As expected, long interconnects have large  $t_d$  due to large  $R_w$  and  $C_w$ . When  $C_E = 10^{-3}$  pF/μm, the SWCNT(6,0) bundle has the smallest  $t_d$  because of its small  $R_w$  (See Fig. 4). As  $C_E$  increases (the feature size decreases), however,  $t_d$  of the SWCNT(24,0) bundle becomes smaller than that of the SWCNT(6,0) bundle because of the small  $C_Q$  of SWCNT(24,0).

## References

- [1] C. Subramaniam *et al.*, *Nat. Commu.* **4**, 3202 (2013)
- [2] <http://quantumwise.com/>
- [3] A. Alizadeh and R. Sarvari, *IEEE Trans. VLSI Syst.* **24**, 2, 803-807 (2016)
- [4] C. Zhan *et al.*, *J. Phys. Chem.* **119**, 22297-22303 (2015)

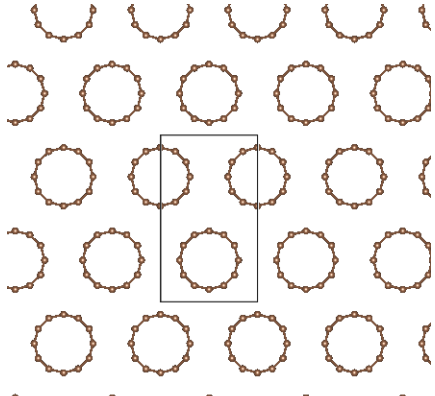


Fig 1. Atomic structure of the SWCNT(6,0) bundle. The black box indicates the primitive unit cell.

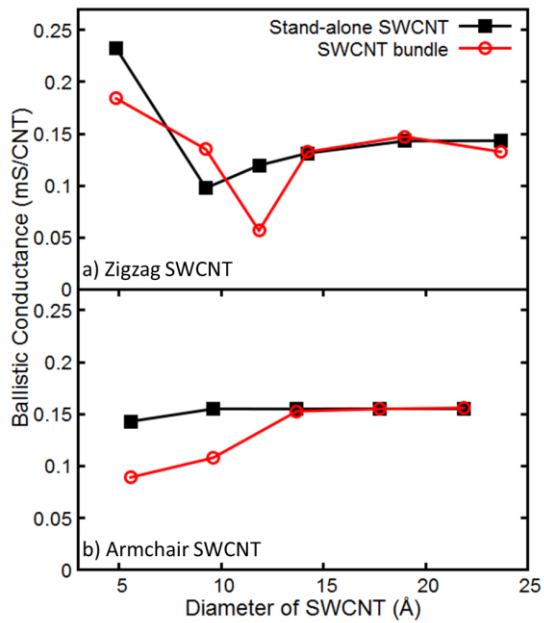


Fig 2. Dependence of  $G_{bal}$  on  $D_{CNT}$  of zigzag and armchair SWCNTs.

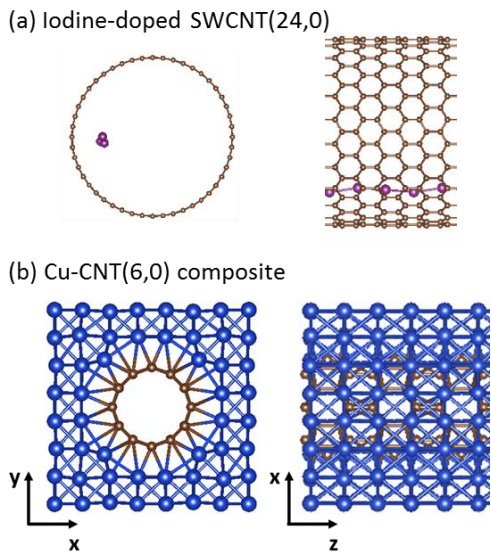


Fig. 3 Atomic structures of the iodine-doped SWCNT and the Cu-CNT composite.

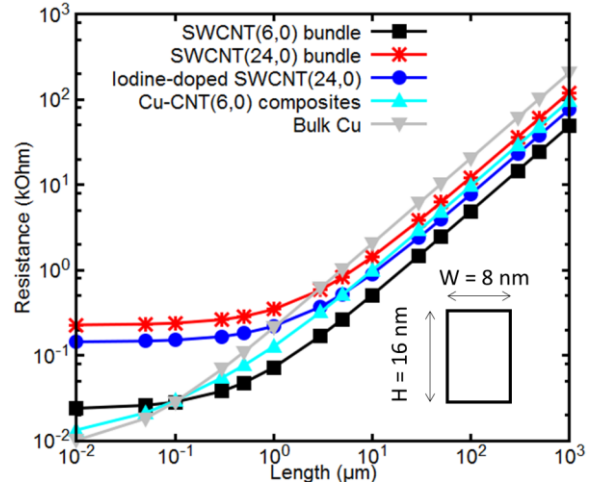


Fig. 4  $R_w$  vs  $L$  with  $W = 8$  nm and  $H = 16$  nm.

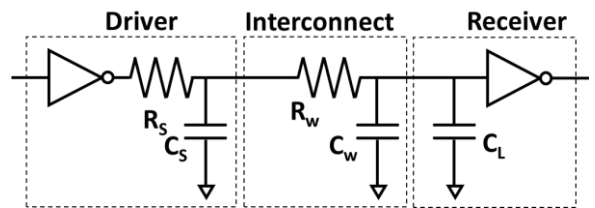


Fig. 5 Schematic representation of a typical interconnect.

Material	$C_Q$ (pF/ $\mu$ m)
SWCNT(6,0) bundle	0.3227
SWCNT(24,0) bundle	0.0146
Iodine-doped SWCNT(24,0)	0.0321
Cu-CNT(6,0)	0.7370
Bulk Cu	0.7821

Table 1.  $C_Q$  of the interconnect with  $W = 8$  nm and  $H = 16$  nm at 300 K.

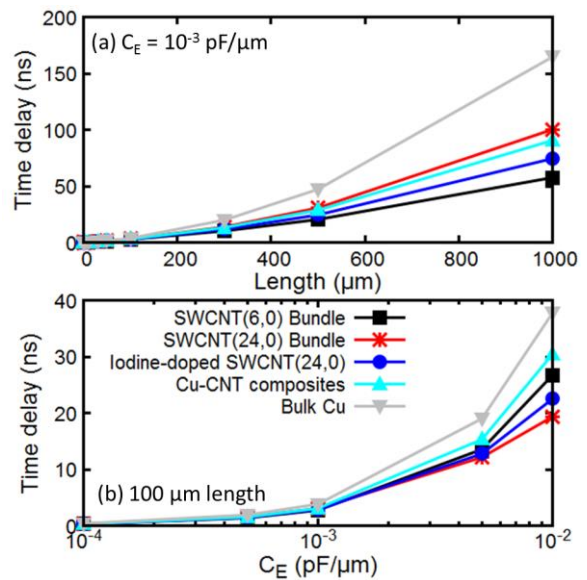


Fig. 6 Dependence of  $t_d$  on  $L$  and  $C_E$ .  $W$  and  $H$  of the interconnect are assumed to be 8 and 16 nm, respectively.